

# Hepatic Extraction Efficiency and Excretion Rate of Technetium-99m-Mebrofenin in Dogs

Gregory B. Daniel, Anne Bahr, Jonathan A. Dykes, Robert DeNovo, Karen Young and Gary T. Smith

*Departments of Small Animal Clinical Sciences and Large Animal Clinical Sciences, College of Veterinary Medicine; Department of Radiology, College of Medicine, University of Tennessee, Knoxville, Tennessee*

Quantitative hepatobiliary scintigraphy aids in the diagnosis of hepatic disease. Two scintigraphic parameters that have great value in discriminating between hepatocellular and biliary disease are hepatic extraction fraction (HEF), which is a measure of the hepatic extraction efficiency (HEE), and hepatic excretion rate. It is generally accepted that hepatic extraction fraction is normally 100%, but a review of the literature provided little information on the actual HEF of  $^{99m}\text{Tc}$ -mebrofenin. **Methods:** We determined the HEE of  $^{99m}\text{Tc}$ -mebrofenin in nine normal dogs after direct injection into the afferent hepatic vasculature using a two-compartment model. The forward and reverse rate constants for the two-compartment model were solved by a simple graphic approach and a more complex numerical approach using a nonlinear least squares algorithm. The HEEs were determined using both methods. **Results:** The HEE for the graphic and numerical methods of analysis were not significantly different and were calculated to be  $92.2 \pm 4.75\%$  (mean  $\pm$  s.d.) and  $91.2 \pm 4.44\%$  (mean  $\pm$  s.d.) by each method, respectively. The half-time clearance of  $^{99m}\text{Tc}$ -mebrofenin was  $19.10 \pm 4.86$  min (mean  $\pm$  s.d.). **Conclusion:** This study validates the assumption that the normal HEE of  $^{99m}\text{Tc}$ -mebrofenin is nearly 100%, barring species differences.

**Key Words:** hepatobiliary scintigraphy; hepatic extraction efficiency; half-time hepatic excretion; technetium-99m-mebrofenin

**J Nucl Med 1996; 37:1846-1849**

Quantitative hepatobiliary scintigraphy (QHS) using  $^{99m}\text{Tc}$ -N-(3-bromo-2,4,6-trimethylacetanilide)-iminodiacetic acid (mebrofenin) is commonly used to evaluate liver disease. Physiologic parameters of hepatic extraction, hepatic excretion, biliary tract patency, and gallbladder contractility can be measured with  $^{99m}\text{Tc}$ -mebrofenin (1). Technetium-99m-mebrofenin enters the hepatocyte through the dye anion receptor by a carrier-mediated, nonsodium-dependent membrane transport mechanism (2). Technetium-99m-mebrofenin does not undergo biotransformation during the transit through the hepatocyte to the bile canaliculus (3,4). The final excretory step involves transportation across the canicular membrane. Hepatocellular disease will decrease both the uptake into hepatocyte and the excretion into the biliary tract (5).

To measure hepatic extraction efficiency (HEE), the hepatobiliary radiopharmaceutical must be extracted from the blood solely by the liver and must be presented to the liver in a single, discrete, intravascular bolus (6-10). Technetium-99m-mebrofenin fulfills the first requirement. Studies in humans have found that 98.1% of  $^{99m}\text{Tc}$ -mebrofenin localized within the liver and excreted into the biliary tract during the 24-hr postinjection period (5). Studies in rats have found that 93.86% of the injected dose will be excreted into the biliary tract (11). The second requirement of single, discrete, intravascular bolus can be overcome by direct injection into the portal vein or

mathematically by deconvolutional analysis after intravenous injection. Calculation of hepatic extraction fraction (HEF) of  $^{99m}\text{Tc}$ -mebrofenin using deconvolutional analysis has been reported in man and dog as a quantitative measure of hepatocyte function (6,8-10,14-16).

The deconvolutional analysis transforms data from an intravenous injection to simulate a direct injection of the radiopharmaceutical into the afferent blood supply of the liver (7,12,13,16). The resultant liver response curve can be used to calculate the HEF. The HEF is derived by dividing the calculated initial hepatic retention, extrapolated from a liver response curve, by the peak vascular activity (5,9,10). Normal HEF of  $^{99m}\text{Tc}$ -mebrofenin is generally considered to be 100% (5). With hepatocellular disease, the HEF will decrease proportional to the severity of liver insult (5,9,10,15). A review of the literature provided little information on the actual HEE of  $^{99m}\text{Tc}$ -mebrofenin. One reference in rats found a first-pass HEE of  $^{99m}\text{Tc}$ -mebrofenin of 74.1% (2). Because of scarce information on the HEE of  $^{99m}\text{Tc}$ -mebrofenin, we determined the HEF of  $^{99m}\text{Tc}$ -mebrofenin in the dog after direct afferent injection into a mesenteric portal vein.

The hepatic excretion rate ( $T_{1/2}$ ) of  $^{99m}\text{Tc}$ -mebrofenin is frequently used to evaluate liver function (1,5,9,10). After intravenous injection, peak liver activity is usually reached within 8-15 min (1,5,17). The excretion phase begins after a brief hepatic transit time. Since the liver receives only 205% of cardiac output from each circulatory pass, there is a continually changing plasma concentration of the radiopharmaceutical after peripheral intravenous injection (18). Some portion of the injected dose of radiopharmaceutical is within the bile canaliculus as other portions are entering the hepatocyte. Because the agent is at different stages of transit thorough the liver, a true hepatic excretion time is difficult to obtain from an intravenous injection. In this study, the entire radiopharmaceutical dose was presented to the liver in a single, discrete bolus, allowing accurate measurement of the true half-time hepatic excretion of  $^{99m}\text{Tc}$ -mebrofenin.

## MATERIALS AND METHODS

Five male and four female adult, conditioned mongrel dogs were obtained from the laboratory animal section of The University of Tennessee, College of Veterinary Medicine. Body weight ranged from 15.9 to 21.36 kg with a mean of 18.94 kg. Preliminary data included physical examination, serum biochemistries, pre- and postprandial bile acids, and BSP retention tests. Ultrasound-guided liver biopsies were taken and submitted for histopathology.

The mebrofenin kits (Choletec, Squibb Diagnostic, Princeton NJ) were reconstituted using the maximum recommended quantity of pertechnetate (100 mCi in 4 ml sterile eluate) to lower the actual milligram quantity of mebrofenin injected. Radiochemical purity was periodically assessed using two ascending chromatographic systems: a silica gel impregnated with instant thin-layer chromatography paper (ITLC-SG) developed with distilled water, and a

Received Aug. 21, 1995; revision accepted Jan. 28, 1996.

For correspondence or reprints contact: Gregory B Daniel, DVM, MS, Department of Small Animal Clinical Sciences, College of Veterinary Medicine, University of Tennessee, PO Box 1071, Knoxville, TN 37901-1071.

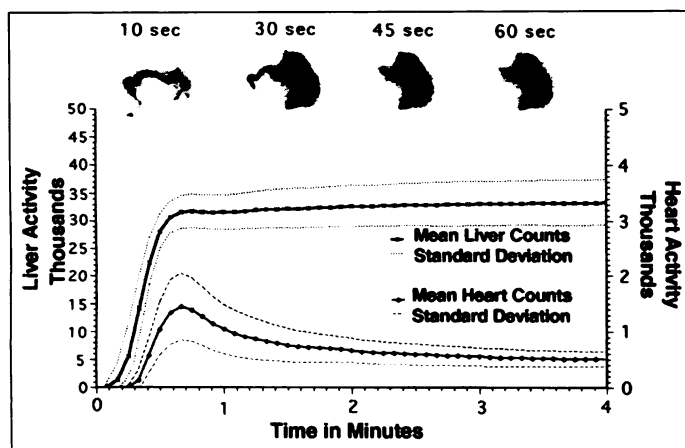


**FIGURE 1.** Serial images at top were obtained after injection of  $^{99m}\text{Tc}$ -mebrofenin in the mesenteric vein. Graph shows the mean and s.d. of the liver and heart counts in nine dogs. Note that different y-axis scales were used to allow visualization of the heart activity. Heart scale, right, is  $1/10^{\text{th}}$  of liver scale, left.

silica acid type instant thin-layer chromatography paper (ITLC-SA) developed with 20% NaCl.

The dogs were premedicated with tiletamine/zolazepam at a dose of 0.5 mg/kg intramuscularly and glycopyrolate at a dose of 0.01 mg/kg intramuscularly to control salivary secretions. Isoflurane anesthesia was administered by mask induction and maintained after tracheal intubation. A ventral midline laparotomy was performed and a segment of jejunum was isolated whereupon a 22-g catheter was placed within a mesenteric vein. The end of the catheter was exteriorized and the segment of bowel replaced into the abdomen. The incision was closed in a routine manner.

The dogs were placed in right lateral recumbent view over a large field of view gamma camera fitted with a low-energy, general-purpose, parallel-hole collimator. Dynamic frame-mode acquisition using a  $64 \times 64 \times 646$  matrix size was controlled by an imaging computer and was initiated simultaneously with injection of the radiopharmaceutical into the mesenteric catheter. The frame rate was 12 frames per minute for 5 min, then 1 frame per minute for an additional 55 min. The mesenteric catheter was removed after scanning and the animal recovered.

The HEE of  $^{99m}\text{Tc}$ -mebrofenin was determined from the dynamic acquisition. Regions of interest (ROIs) were drawn around the entire liver and heart. The total number of counts in each organ was plotted to create time-activity curves (Fig. 1). The heart time-activity data were used to represent blood-pool activity and the liver time-activity data were used to represent hepatocyte activity plus the portion of the blood pool in the liver vascular space.

We used a two-compartment model (Fig. 2) to determine HEE from ROI measurements of blood-pool and hepatic time-activity data. In the model depicted,  $C_p$  represents blood-pool activity

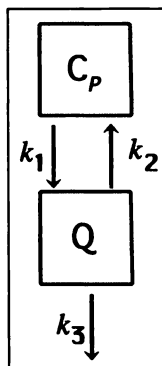


**FIGURE 2.** Schematic drawing of a two-compartment model. Compartment  $C_p$  represents blood-pool activity and  $Q$  represents hepatocyte activity. Forward and reverse rate constants between blood pool and hepatocytes are designated as  $k_1$  (1/min) and  $k_2$  (1/min), respectively, and  $k_3$  (1/min) is the rate constant for the irreversible process between hepatocytes and the biliary tree.

(cpm) and  $Q$  represents hepatocyte activity (cpm). The model differential equation can be written:

$$\dot{Q} = -(k_2 + k_3)Q + k_1 C_p, \quad \text{Eq. 1}$$

where  $k_1$  (1/min) and  $k_2$  (1/min) are the forward and reverse rate constants between blood pool and hepatocytes, respectively, and  $k_3$  (1/min) is the rate constant for the irreversible process between hepatocytes and the biliary tree. During the first three minutes after injection of the tracer, the effects of hepatocyte to bile transit was assumed to be negligible, i.e.  $k_3$  is fixed at zero. If a longer times interval were used, i.e., greater than 3 min, the effect of  $k_3$  would have to be considered in the analysis. The measured activity in the liver ROI,  $Y$ , actually represents the sum of both hepatocyte activity and a fraction of blood-pool activity:

$$Y = Q + VC_p, \quad \text{Eq. 2}$$

where  $V$  is the vascular fraction contained within the liver time-activity data. The HEE was defined as the ratio of extracted activity to the total activity entering the system (19):

$$\text{HEE} = \frac{\int Q}{\int Q + \int C_p} \quad \text{Eq. 3}$$

Since  $Q$  is unknown, the numerical solution for Equation 1 is necessary to solve for HEE. Assuming equilibrium between  $C_p$  and  $Q$  shortly after injection (i.e.  $\dot{Q} = 0$ ), then it is evident from Equation 1 that:

$$k_1 C_p = k_2 Q \quad \text{Eq. 4}$$

Integrating Equation 4 and combining with Equation 3 yields the following result for the HEE:

$$\text{HEE} = \frac{k_1}{k_1 + k_2} \quad \text{Eq. 5}$$

The HEE value can be determined if estimates of  $k_1$  and  $k_2$  can be obtained from the dynamic time-activity data. If the system is not assumed to be in equilibrium, the resulting expression for HEE is:

$$\text{HEE}_{\text{corr}} = \frac{k_1 - \phi}{k_1 + k_2 - \phi} \quad \text{Eq. 6}$$

where  $\phi = Q/\int C_p$  and  $\text{HEE}_{\text{corr}}$  is the corrected extraction efficiency. The resulting value for  $\text{HEE}_{\text{corr}}$  can be obtained once  $k_1$  and  $k_2$  and  $V$  are known.

We used two approaches to estimate the rate constants: a graphical method using linearized time-activity data, and direct numerical solutions to the model differential equations using a nonlinear least squares algorithm. Solving Equation 2 for  $Q$  (and by differentiating with respect to time) and substituting the result(s) into Equation 1 gives the linearized expression:

$$\frac{Y}{C_p} = -k_2 \frac{\int Y}{C_p} + (k_1 + k_2 V) \frac{\int C_p}{C_p} + V. \quad \text{Eq. 7}$$

This expression is similar to the Patlak equation used in PET imaging (20). Solution of Equation 6 for the slopes,  $m1 = -k_2$ ,  $m2 = k_1 + k_2 V$ , and the intercept,  $b = V$ , is simple with multiple linear regression analysis available on microcomputer spreadsheet software available today (21). Algebraic solution for  $k_1$ ,  $k_2$  and  $V$  is then possible. Numerical solution of Equations 1 and 2 yield direct estimates of  $k_1$ ,  $k_2$  and  $V$ . Substitution of  $k_1$ ,  $k_2$  and  $V$  estimates into Equations 5 or 6 yields the desired estimates for HEE and  $\text{HEE}_{\text{corr}}$ . We used only the first 3 min of time-activity data for the graphical solution, and both the first three minutes and up to 60 min for the numerical solutions ( $\text{HEE}_{\text{numerical}}$ ).

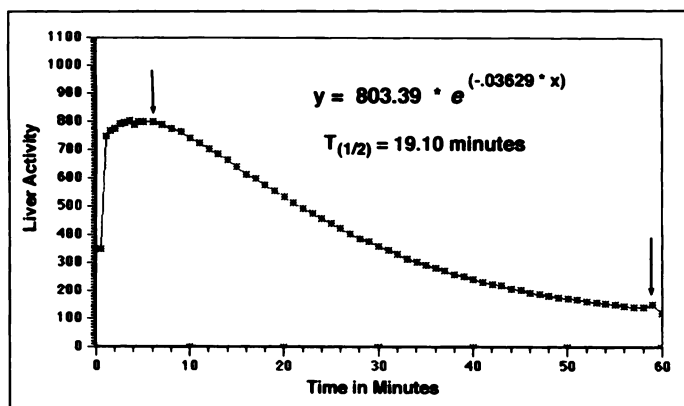


**FIGURE 3.** Liver time-activity curves out to 60 min postinjection into a mesenteric portal venous catheter. Average count density from four peripherally drawn liver regions was determined for each dog. Graphs show mean liver count densities for all nine dogs. Nonlinear least squares approximation was fitted to the downslope portion of the curve between the two arrows. Regression formula and  $T_{1/2}$  are provided for the given curve.

For calculation of hepatic excretion, ROIs were drawn over four areas of the liver; ROI 1 along the caudal ventral liver margin, ROI 2 over the caudal dorsal liver margin, ROI 3 over the cranial ventral liver margin and ROI 4 over the cranial dorsal liver margin. All images of the acquisition were carefully inspected to ensure that the ROIs did not overlap a major biliary duct. The mean count density of all four liver regions was plotted. A nonlinear least squares fit of the liver curve was made from the beginning of the down slope of the curve to the 60-min time point using the following formula (Fig. 3):

$$Y = A * e^{-\lambda x} \quad \text{Eq. 8}$$

### Statistical Analysis

A one-way analysis of variance was performed on the HEE results from the numerical method and corrected and uncorrected graphical methods. All tests had a level of significance of  $p < 0.05$ .

### RESULTS

All dogs were considered normal based on serum biochemistries, bile acids and BSP retention times and liver histopathology. (Table 1) The animals were injected with  $3.33 \pm 0.24$  mCi (mean  $\pm$  s.d.)  $^{99m}\text{Tc}$  labeled to  $1.69 \pm 0.31$  mg (mean  $\pm$  s.d.) of mebrofenin. The radiochemical purity of the radiopharmaceutical was  $97.71 \pm 0.77\%$  (mean  $\pm$  s.d.) of  $^{99m}\text{Tc}$  bound to mebrofenin with  $0.60 \pm 0.58\%$  (mean  $\pm$  s.d.) as  $^{99m}\text{TcO}_4^-$  and  $1.68 \pm 0.43\%$  as reduced  $^{99m}\text{Tc}$ .

The results of the compartmental analyses are shown in Table 2. Absolute values of the rate constants  $k_1$  and  $k_2$ , and the

**TABLE 1**  
Result of Serum Chemistries

Serum	
Total protein (g/dl)	$7.20 \pm 0.54$
Bilirubin (mg/dl)	$0.24 \pm 0.10$
Alkaline phosphatase (IU/liter)	$50.33 \pm 24.92$
ALT (IU/liter)	$29.78 \pm 10.10$
AST (IU/liter)	$19.67 \pm 6.15$
BSP (%)	$2.93 \pm 0.97$
Pre-BA ( $\mu\text{M/liter}$ )	$6.99 \pm 7.43$
Post-BA ( $\mu\text{M/liter}$ )	$7.66 \pm 5.94$

ALT = alanine aminotransferase; AST = aspartate aminotransferase; BSP = sulfobromophthalein; Pre-Ba = fasting bile acids; Post-Ba = postprandial bile acids.

**TABLE 2**

HEE Derived from Differential Equation Analysis of a Two-Compartment Model

HEE	HEE <sub>corr</sub>	HEE <sub>numerical</sub>
$95.7\% \pm 2.56\%$	$92.2\% \pm 4.75\%$	$91.2\% \pm 4.44\%$

distribution volume,  $V$ , are dependent on physical parameters such as attenuation in the ROI and, therefore, are not included in the table. The HEE, is independent of these parameters.

The estimated HEE using graphical analysis and assuming equilibrium conditions (Eq. 5) was  $95.7 \pm 2.56\%$  (mean  $\pm$  s.d.). HEE assuming nonequilibrium conditions, HEE<sub>corr</sub>, was calculated to be  $92.2 \pm 4.75\%$  (mean  $\pm$  s.d.). This result corresponded to HEE<sub>numerical</sub> calculated from nonlinear numerical analysis of  $91.2 \pm 4.44\%$  (mean  $\pm$  s.d.). There was no significant difference between the HEE<sub>corr</sub> and the HEE<sub>numerical</sub> ( $p < 0.05$ ). HEE, assuming equilibrium conditions, was significantly different from both the HEE<sub>corr</sub> and HEE<sub>numerical</sub> ( $p < 0.024$ ). Comparison of the corrected graphical data to the numerical analysis yielded the same straight line relationship ( $y = 1.03x - 0.02$ ,  $r^2 = 0.92$ ).

Liver activity began to decrease after five minutes. The clearance appeared to fit a single exponential model. The half-time clearance ( $T_{1/2}$ ) of the radiopharmaceutical was  $19.10 \pm 4.86$  min (mean  $\pm$  s.d.).

### DISCUSSION

Direct measurement of first-pass HEE requires injection into the afferent blood supply of the liver with quantitation of the hepatic outflow activity (2,6). Since the liver has a dual blood supply, an afferent injection could be made through either the portal vein or hepatic arteries (23). We chose to administer the  $^{99m}\text{Tc}$ -mebrofenin into the portal vein through mesenteric venous catheterization. Intra-arterial injection in the hepatic arteries was attempted but abandoned. Because of the numerous hepatic branches off the celiac artery, a branch catheterization could not ensure radiopharmaceutical delivery to all regions of the liver. If an intra-arterial catheter is placed deeply into a hepatic branch of the celiac artery, only a portion of the liver would receive the radiopharmaceutical. If the catheter was placed proximally in the celiac artery, a portion of the radiopharmaceutical dose would flow to the abdominal viscera before reaching the liver. If a portion of the radiopharmaceutical dose entered the left gastric artery (which is in close proximity to the hepatic branches), some of the radiopharmaceutical could, theoretically, bypass the liver through the esophageal artery which empties into the systemic venous return. This would result in a artifactually low HEE.

The mesenteric portal venous injection delivered the radiopharmaceutical uniformly throughout the liver in all nine dogs. Since the portal and arterial blood supply mix together in the lateral portions of the liver lobules before they enter the hepatic sinusoids, either method would provide an afferent administration of the radiopharmaceutical to the liver.

An imaging computer was used to quantify the activity within the liver and heart. A two-compartment model was used to describe the data. The forward ( $k_1$ ) and reverse ( $k_2$ ) rate constants could be determined by a simple graphical method using linearized time-activity data. The graphical approach yielded a calculated extraction fraction of 92.2% for the nine dogs when corrected for nonequilibrium conditions. The HEE<sub>corr</sub> determined from this graphical method correlated well with the more complex direct numerical solutions to the model

using a nonlinear least squares algorithm. The graphical method is simple to implement in a clinical environment by using existing spreadsheet software in place of otherwise complex nonlinear parametric analysis software. Both methods found a first pass HEF of  $^{99m}\text{Tc}$ -mebrofenin to be 91%–92%.

The HEF is an approximation of the HEE and is used as an objective measure of hepatocellular function. The method described in this paper to calculate HEE is not clinically applicable but HEF is and can be obtained after intravenous injection by using deconvolutional analysis. Deconvolutional analysis provides a fast, noninvasive method that can be used in clinical situations to provide a dynamic assessment of hepatocyte function. Clinical applications of HEF could include differentiation of hepatocellular dysfunction from early biliary disease. It is not uncommon to not fully visualize the biliary tree in the presence of severe, acute hepatocyte dysfunction. In these cases, deconvolutional analysis can aid in separating severe hepatocellular disease from extrahepatic obstructions which require surgery. In patients with hepatocellular disease, the HEF will be decreased, whereas in cases of early extrahepatic biliary obstruction, the HEF is expected to be normal (15). Hepatic extraction fractions have been useful in evaluation of liver transplantations, where early detection of changes in liver function are crucial to avert organ rejection (6,5,14). We are currently measuring HEF in dogs with toxin-induced liver dysfunction.

## CONCLUSION

Technetium-99m-mebrofenin is commonly used for quantitative hepatobiliary scintigraphy because of its high HEE and rapid hepatic clearance (1,5,11,22). This study validates the assumption that normal HEE of  $^{99m}\text{Tc}$ -mebrofenin is nearly 100%, barring species differences. The  $T_{1/2}$  for hepatic excretion was 19.10 min, which is similar to other reported values (17). Our findings support the 90%–100% HEF obtained with deconvolutional analysis after intravenous injection of  $^{99m}\text{Tc}$ -mebrofenin in normal subjects (16).

## ACKNOWLEDGMENT

This work was supported by a grant from Hills Pet Nutrition, Inc., Topeka, KS.

## REFERENCES

1. Krishnamurthy GT, Turner FE. Pharmacokinetics and clinical application of technetium-99m-labeled hepatobiliary agents. *Semin Nucl Med* 1980;20:130–149.
2. Fritzberg AR. Advances in the development of hepatobiliary radiopharmaceuticals. In: Fritzberg AR, ed. *Radiopharmaceuticals: Progress and clinical perspectives*, vol. 1. Boca Raton: CRC Press; 1986: 90–116.
3. Loberg MD, Cooper M, Harvey E, et al. Development of new radiopharmaceutical based on N-substitution of iminodiacetic acid. *J Nucl Med* 1976;17:633–638.
4. Loberg MD, Fields AT. Chemical structures of Tc-99m-labeled N-(2,6 dimethylphenylcarbamoylmethyl) iminodiacetic acid (Tc-HIDA). *Int J Appl Radiat Isot* 1978;29: 167–173.
5. Doo E, Krishnamurthy GT, Eklem MJ, Gilbert S, Brown pH. Quantification of hepatobiliary function as an integral part of imaging with technetium-99m-mebrofenin in health and disease. *J Nucl Med* 1991;32:48–57.
6. Tagge EP, Campbell DA, Reichle R, et al. Quantitative scintigraphy with deconvolutional analysis for the dynamic measurement of hepatic function. *J Surg Res* 1987;42:605–612.
7. Juni JE, Thrall JH, Froelich JW, et al. The appended curve technique for deconvolutional analysis - method and validation. *Eur J Nucl Med* 1988;14:403–407.
8. Howman-Giles R, Moase A, Gaskin K, Uren R. Hepatobiliary scintigraphy in a pediatric population: determination of hepatic extraction fraction by deconvolutional analysis. *J Nucl Med* 1993;34:214–221.
9. Brown pH, Juni JE, Lieberman DA, Krishnamurthy GT. Hepatocyte versus biliary disease: a distinction by deconvolutional analysis Tc-99m IDA time-activity curves. *J Nucl Med* 1988;29:623–630.
10. Lieberman DA, Brown pH, Krishnamurthy GT. Improved scintigraphic assessment of severe cholestasis with the hepatic extraction fraction. *Dig Dis Sci* 1990;35:1385–1390.
11. Nunn AD, Loberg MD, Conley RA. A structure-distribution-relationship approach leading to the development of Tc-99m-mebrofenin: an improved cholescintigraphic agent. *J Nucl Med* 1983;24:423–430.
12. Juni JE, Reichle R, Pitt S. Quantitative measurement of hepatic artery and portal vein blood flow by deconvolution analysis [Abstract]. *J Nucl Med* 1986;27:957.
13. Williams DL. Improvement in quantitative data analysis by numerical deconvolution techniques. *J Nucl Med* 1979;20:568–569.
14. Heyman S. Hepatobiliary scintigraphy as a liver function test. *J Nucl Med* 1994;35: 436–437.
15. Juni JE, Reichle R. Measurement of hepatocellular function with deconvolutional analysis: application in the differential diagnosis of acute jaundice. *Radiology* 1990;177:171–175.
16. Bahr A, Daniel GB, DeNovo R, et al. Quantitative hepatobiliary scintigraphy with deconvolutional analysis for the measurement of hepatic function in dogs. *Vet Radiol and Ultras* 1996;37:214–220.
17. Kerr LY, Hornof WJ. Quantitative hepatobiliary scintigraphy using Tc-99m-DISIDA in the dog. *Vet Radiology Ultrasound* 1986;27:173–177.
18. Center SA, Strombeck DR. Liver: normal function and physiology. In: Guildford WG, Center SA, Strombeck DA, Myers DJ, eds. *Strombeck's small animal gastroenterology*, 2nd ed. Philadelphia: WB Saunders; 1996.
19. Huang SC, Phelps ME. Principles of tracer kinetic modeling in PET and autoradiography. In: Phelps ME, Mazziotta J, Schelbert HR, eds. *Positron emission tomography and autoradiography*. New York, NY: Raven Press; 1986:287–346.
20. Patlak CS, Blasberg RG, Fenstermacher JD. Graphical evaluation of blood-to-brain transfer constants from multiple-time uptake data. *J Cereb Blood Flow Metab* 1983;3:1–7.
21. Thie JA, Smith GT, Hubner KF. Total graphical analysis of dynamic PET data with identification of up to four parameters [Abstract]. *J Nucl Med* 1993;34:185P.
22. Krishnamurthy S, Krishnamurthy GT. Technetium-99m-iminodiacetic acid organic anions: review of biokinetics and clinical application in hepatology. *Hepatology* 1989;9:139–153.
23. Evans HE. The heart and arteries. In: Evans HE, ed. *Miller's anatomy of the dog*, 3rd ed. Philadelphia, PA: WB Saunders Co.; 1993:586–681.